

# Designing good bosonic quantum codes via creating destructive interference

Linshu Li,<sup>1</sup> Dylan J. Young,<sup>1</sup> Victor V. Albert,<sup>1,2</sup> Kyungjoo Noh,<sup>1</sup> Chang-Ling Zou,<sup>1,3</sup> and Liang Jiang<sup>1</sup>

<sup>1</sup>*Yale Quantum Institute, Departments of Applied Physics and Physics, Yale University, New Haven, CT 06511, USA*

<sup>2</sup>*Walter Burke Institute for Theoretical Physics and Institute for Quantum Information and Matter, California Institute of Technology, Pasadena, California 91125, USA*

<sup>3</sup>*Key Laboratory of Quantum Information, University of Science and Technology of China, Hefei, Anhui 230026, China*

Continuous-variable systems protected by bosonic quantum error-correcting codes have emerged as a promising platform for quantum information processing. To date, design of codewords has centered on optimizing the occupation of basis states in the error-relevant basis. Here, we propose utilizing the phase degree of freedom in basis state probability amplitudes to devise codes that feature destructive interference, and thus reduced overlap, between error codewords. To showcase, we first consider the correction of excitation loss using single-mode codes with Fock-space parity structure and show that, with a tailored “two-level” recovery, altering the signs of probability amplitudes can significantly suppress decoherence. We then study the joint channel of excitation loss and Kerr effect, and show the critical role of nontrivial phase for optimal quantum codes for such channels. The principle is extended to improve bosonic codes defined in other bases and multi-qubit codes, showing its broader applicability in quantum error correction.

*Introduction* Quantum operations with continuous variables represent a promising alternative path towards scalable quantum computing and communication [1–4]. Similar to qubit-based systems, a major challenge for faithful bosonic quantum information is to store, manipulate and communicate the encoded information in the presence of noise, such as excitation loss (aka amplitude damping, pure loss), phase-space drift, dephasing and cavity nonlinearities. To overcome excitation loss that fundamentally limits the cavity lifetime, multi-mode codes were first introduced [5–9]; for phase-space drift, Gottesman, Kitaev, and Preskill (gkp) codes [3, 10] were proposed. More recently, motivated by the potential to utilize higher excitation states in a bosonic Hilbert space and perform hardware-efficient operations, single-mode codes for excitation loss such as `cat` codes [11–15] and binomial (`bin`) codes [16] were developed. Meanwhile, progress in superconducting circuit quantum electrodynamics (QED) [17–19] – e.g. FPGA adaptive control [13], readout of excitation parity [17] and universal control of cavity states [18, 19] – has opened up possibilities once thought unreachable, including implementing arbitrary quantum channels on a bosonic mode [20, 21]. With the advances, error-corrected `cat` and `bin` qubits and the associated universal quantum gate sets have been demonstrated, respectively [13, 22, 23]. These capabilities are essential for higher-level operations such as distributing error-corrected entangled states [24] and quantum gate teleportation [25].

For the aforementioned codes, in the computational basis relevant to the error under consideration, i.e. Fock basis for `cat/bin` codes and position/momentum basis for square-lattice gkp codes, the codewords are spanned by distinct subsets of basis states with positive probability amplitudes. Recently, gkp codes have been found to protect against excitation loss extremely well, even though they were not originally designed for loss errors

[26, 27]. Similar to the newly discovered numerically optimized codes [16, 26], when expressed in the Fock basis, their codewords do not possess parity structure, yet feature negative probability amplitudes. The findings inspire us to better understand the recipe behind desirable quantum error-correction (QEC) capabilities and generalize the findings to devise more efficient codes.

In this Letter, we explore the conjugate degree of freedom to basis state occupation – the relative phases – and demonstrate its critical role for efficient quantum codes. Firstly, we show that tuning the phase degree of freedom in the codewords can improve code performance via making error codewords interfere destructively. As illustrations, concerning the correction of excitation loss, we modify `bin` and `cat` codes by periodically altering the signs of probability amplitudes in one codeword, and show that the sign alteration (SA) effectively reduces the overlap between selected error codewords. The periodic SA can be experimentally realized via adding a cavity Kerr to the encoding procedure. To capture the enhanced separation created by SA, we propose a two-level recovery that yields error protection close to optimal at loss rates of practical interest. The enhancement naturally leads to a question: Is phase degree of freedom necessary for *optimal* code constructs? Using biconvex optimization of encoding and decoding [27–29], we compute the optimal code given an error process and find that, although nontrivial phase (neither 0 nor  $\pi$ ) is redundant for excitation loss, it is necessary for more complicated ones such as the joint channel of excitation loss and Kerr effect.

Extending the principle to codes defined in bases beyond Fock, we note that GKP codes over non-square lattices, which better overcome phase-space drift than square lattice GKP, can be generated from the later through SA in position-momentum basis [3]. In addition, noting that well-known multi-qubit CSS codes [30–32]

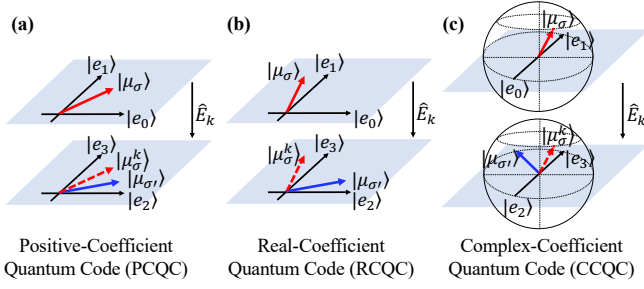


Figure 1. Illustrations of error codeword overlap for (a) positive-coefficient, (b) real-coefficient and (c) complex-coefficient quantum code. Here,  $|\mu_\sigma\rangle$  are codewords and  $|e_i\rangle$  are computational basis states that span  $|\mu_\sigma\rangle$ . By allowing (b)  $\theta_n^\sigma = 0, \pi$  and (c)  $\theta_n^\sigma \in [0, 2\pi)$ , after the occurrence of  $\hat{E}_k$  to  $|\mu_\sigma\rangle$  (red solid vector), error codeword  $|\mu_\sigma^k\rangle$  (red dashed vector), spanned by the same  $S_{\sigma'}$  as another codeword  $|\mu_{\sigma'}\rangle$  (blue vector), remains largely separable from  $|\mu_{\sigma'}\rangle$  due to destructive interference. For clarity, we assume each codeword consists of two basis states.

share the same feature of all positive probability amplitudes with **bin** and **cat** codes, we modify the nine-qubit Shor code for enhanced protection against Pauli errors and amplitude damping error, demonstrating the wide applicability of the principle for enhanced quantum error correction.

*Principle* We begin with introducing the principle that engineering the phase degree of freedom in codewords can create destructive interference between them after error, thus suppressing undesired overlap. Given a qudit code embedded in a Hilbert space  $\mathcal{H} = \{|n\rangle\}$  where  $n$  indexes computational basis states, normalized codewords in a chosen logical basis can be written as

$$|\mu_\sigma\rangle = \sum_{n \in S_\sigma} c_n^\sigma e^{i\theta_n^\sigma} |n\rangle \quad (1)$$

where  $\sigma = 0, 1, \dots, d-1$  labels codewords,  $c_n^\sigma > 0$  and  $S_\sigma$  is a subset of the computational basis chosen for each codeword. The error process that the code in Eq. (1) is devised to protect against can be expressed in the Kraus representation  $\mathcal{E}(\rho) = \sum_k \hat{E}_k \rho \hat{E}_k^\dagger$ , with each operator  $\hat{E}_k$  associated with an error event. The decoherence under  $\mathcal{E}$  is captured by the QEC matrix  $M_{kl, \sigma\sigma'} = \langle \mu_\sigma | \hat{E}_k^\dagger \hat{E}_l | \mu_{\sigma'} \rangle$  [33, 34], i.e. overlap between codewords under errors, and

$$\langle \mu_\sigma | \hat{E}_k^\dagger \hat{E}_l | \mu_{\sigma'} \rangle = \sum_{m, n} c_m^\sigma c_n^{\sigma'} e^{i(\theta_n^{\sigma'} - \theta_m^\sigma)} \langle m | \hat{E}_k^\dagger \hat{E}_l | n \rangle. \quad (2)$$

We see that, depending on the nature of error and its relation to the computational basis, magnitude  $c_n^\sigma$  and phase  $\theta_n^\sigma$  are both critical in suppressing Eq. (2).

Figure 1 illustrates how phase allows codewords, after an error occurs, to remain distinguishable. Fig. 1(a) shows the case of *positive-coefficient quantum code* (PCQC), for which  $\theta_n^\sigma = 0$  and it relies only on  $c_n^\sigma$  and a

wise choice of  $S_\sigma$  to ensure orthogonality between codewords and QEC capacity. Examples include **bin**, **cat**, multi-mode [5, 6], square-lattice **gkp** codes for phase-space drift and multi-qubit CSS codes. Once error  $\hat{E}_k$  takes  $|\mu_\sigma\rangle$  to the subspace  $|\mu_{\sigma'}\rangle$  lies in,  $|\mu_{\sigma'}\rangle$  and error word  $|\mu_\sigma^k\rangle := \hat{E}_k |\mu_\sigma\rangle / \sqrt{\langle \mu_\sigma | \hat{E}_k^\dagger \hat{E}_k | \mu_\sigma \rangle}$  will overlap, inducing decoherence. However, if we consider a *real-coefficient quantum code* (RCQC) where  $\theta_n^\sigma \in \{0, \pi\}$  [Fig. 1(b)], or even *complex-coefficient quantum code* (CCQC) where  $\theta_n^\sigma \in [0, 2\pi)$  [Fig. 1(c)], dependent on the error under consideration and selected computational basis, larger separation between  $|\mu_\sigma^k\rangle$  and  $|\mu_{\sigma'}\rangle$  can potentially be realized due to destructive interference between basis states. Without losing generality, we focus on quantum codes that encode a qubit.

To see how better codes can emerge as a result, we begin with a neat example – the bosonic  $\sqrt{17}$ -code [16] – that corrects a single loss without a parity structure key to other codes

$$|0_L\rangle = \frac{1}{\sqrt{6}} (\sqrt{7 - \sqrt{17}} |0\rangle + \sqrt{\sqrt{17} - 1} |3\rangle), \quad (3)$$

$$|1_L\rangle = \frac{1}{\sqrt{6}} (\sqrt{9 - \sqrt{17}} |1\rangle - \sqrt{\sqrt{17} - 3} |4\rangle). \quad (4)$$

$\hat{a}|0_L\rangle$  ( $\hat{a}$  is annihilation operator) and  $|1_L\rangle$ , spanned by different Fock states, do not overlap. Meanwhile, one can test that, due to *destructive interference*,  $\hat{a}|1_L\rangle \propto \sqrt{9 - \sqrt{17}} |0\rangle - 2\sqrt{\sqrt{17} - 3} |3\rangle$  is also orthogonal to  $|0_L\rangle$ , thus allowing the code to fully correct one excitation loss.

*Sign-altered bin code for excitation loss* The energy decay of an oscillator is described by excitation loss channel  $\mathcal{N}_\gamma$  ( $\gamma$  is loss rate), for which Kraus operator  $\hat{E}_k = \sqrt{\frac{\gamma^k}{k!}} (1 - \gamma)^{\frac{n}{2}} \hat{a}^k$  [5, 15, 16] ( $\hat{n} = \hat{a}^\dagger \hat{a}$  is the excitation number operator) is associated with losing  $k$  excitations. To correct the multi-loss events, based on **bin**( $N, S$ ) that corrects exactly  $S - 1$  losses for  $N \geq S$

$$|0_{\text{bin}}/1_{\text{bin}}\rangle = 2^{-\frac{N-1}{2}} \sum_{p \text{ even/odd}}^{[0, N]} \sqrt{\binom{N}{p}} |pS\rangle, \quad (5)$$

we apply a periodic SA to  $|0_{\text{bin}}\rangle$  while keeping those of  $|1_{\text{bin}}\rangle$  unchanged, and obtain sign-altered binomial (**sab**) code with

$$|0_{\text{sab}}\rangle = 2^{-\frac{N-1}{2}} \sum_{p \text{ even}}^{[0, N]} (-1)^{\frac{p}{2}} \sqrt{\binom{N}{p}} |pS\rangle, \quad (6)$$

and  $|1_{\text{sab}}\rangle = |1_{\text{bin}}\rangle$ . With the same parity structure, **sab**( $N, S$ ) code also corrects  $S - 1$  losses perfectly as **bin**( $N, S$ ). The advantage emerges when we examine higher-order QEC matrix entries  $\langle \mu_\sigma | \hat{E}_k^\dagger \hat{E}_{S+k} | \mu_{\sigma'} \rangle$  ( $k = 0, 1, \dots$ ): Here, the  $(-1)^{\frac{p}{2}}$  in Eq. (6) leads to destructive interference between the two error codewords, reducing the overlap responsible for logical-X error.

The encoding procedure of **sab** code builds on that of **bin** code with an additional Kerr unitary that imprints SA to  $|0_{\text{bin}}\rangle$  while acting trivially on  $|1_{\text{bin}}\rangle$  as a result of the parity structure. To see this, we first introduce Kerr unitary  $\hat{U}_{\text{Kr}} = e^{\frac{1}{2}iKt\hat{n}^2}$  with strength coefficient  $K$ . Denoting  $\hat{U}_S = \exp[i\pi\hat{n}^2/(2S)^2]$ , we see that

$$\hat{U}_S|0_{\text{bin}}\rangle = |0_{\text{sab}}\rangle, \quad \hat{U}_S|1_{\text{bin}}\rangle = e^{i\frac{\pi}{4}}|1_{\text{sab}}\rangle. \quad (7)$$

Note that  $e^{i\frac{\pi}{4}}$  can be removed by redefining  $|1_{\text{sab}}\rangle$ . Hence the encoding of **sab** is realized as  $\mathcal{S}_{\text{sab}}(\cdot) = \hat{U}_S\mathcal{S}_{\text{bin}}(\cdot)\hat{U}_S^\dagger$ .

*Two-level recovery* A complete QEC process is described by the effective qubit channel  $\mathcal{E} = \mathcal{S}^{-1} \circ \mathcal{R} \circ \mathcal{N} \circ \mathcal{S}$  that consists of encoding  $\mathcal{S}$ , error channel  $\mathcal{N}$ , recovery  $\mathcal{R}$  and decoding  $\mathcal{S}^{-1}$  [26]. Given  $\mathcal{S}$  and  $\mathcal{N}$ , the code performance then depends on choice of  $\mathcal{R}$  – in the case of **sab**, we need to design an  $\mathcal{R}$  that effectively captures the enhanced separation between error codewords.

We first recall the recovery proposed for equally-spaced codes with spacing  $S$  [15–17]. The recovery  $\mathcal{R}^{(1)} = \{\hat{R}_0^{(1)}, \hat{R}_1^{(1)}, \dots, \hat{R}_{S-1}^{(1)}\}$  and Kraus operator  $\hat{R}_i^{(1)} = \hat{U}_i^{(1)}\hat{\Pi}_{i \bmod S}$  where  $\hat{\Pi}_{i \bmod S}$  is the projection operator into the subspace with excitation number  $i$  modulo  $S$ , and unitary  $\hat{U}_i^{(1)}$  performs state transfer  $|\mu_\sigma^{(S-i) \bmod S}\rangle \leftrightarrow |\mu_\sigma\rangle$ .  $\mathcal{R}^{(1)}$  makes use of the parity structure to correct the first  $S-1$  excitation losses, and losses beyond the first  $S-1$  will lead to bit-flip error. As such, here we call it “one-level” recovery.

To capture the enhanced error codeword separation, we propose a new recovery  $\mathcal{R}^{(2)}$  that, in addition to correcting the first  $S-1$  losses, exploits the component in error word  $|\mu_\sigma^{S+k}\rangle$  that is orthogonal to  $|\mu_\sigma^k\rangle$  ( $k = 0, 1, \dots, S-1$ ), i.e.  $|\mu_\sigma^{S+k}\rangle - \langle\mu_\sigma^k|\mu_\sigma^{S+k}\rangle|\mu_\sigma^k\rangle$ . Since events with  $S$  to  $2S-1$  losses are also partially corrected, we call  $\mathcal{R}^{(2)}$  “two-level” recovery [26]. We note that  $\mathcal{R}^{(2)}$  improves the performance of **bin** compared to  $\mathcal{R}^{(1)}$  [26], yet the enhancement is much more pronounced for **sab** due to the intentionally enlarged separation between  $|\mu_\sigma^{S+k}\rangle$  and  $|\mu_\sigma^k\rangle$ .

The 1<sup>st</sup> level of  $\mathcal{R}^{(2)}$ , similarly to  $\mathcal{R}^{(1)}$  [16], fully corrects the first  $S-1$  losses. Each Kraus operator consists of a projection and a restoring unitary

$$\hat{R}_k^{(2)} = \sum_\sigma (|\mu_\sigma^k\rangle\langle\mu_\sigma^k| + \hat{U}_k^{\text{res}})\hat{P}_k. \quad (8)$$

Here,  $k = 0, 1, \dots, S-1$ ,  $\hat{P}_k = \sum_\sigma |\mu_\sigma^k\rangle\langle\mu_\sigma^k|$  projects to each error subspace, and  $\hat{U}_k^{\text{res}}$  finishes the unitary rotation in  $\text{Span}\{|\mu_\sigma\rangle, |\mu_\sigma^k\rangle\}$  – for  $k \neq 0$ , it is simply  $|\mu_\sigma^k\rangle\langle\mu_\sigma|$ .

Also,  $\mathcal{R}^{(2)}$  has a 2<sup>nd</sup> level with  $S$  Kraus operators

$$\hat{R}_{S+k}^{(2)} = \sum_\sigma (|\mu_\sigma^k\rangle\langle\mu_\sigma^k| + \hat{U}_{S+k}^{\text{res}})\hat{P}_{S+k} \quad (9)$$

where, for  $k = 0, 1, \dots, S-1$ , the normalized  $|\nu_\sigma^k\rangle \propto |\mu_\sigma^{S+k}\rangle - \langle\mu_\sigma^k|\mu_\sigma^{S+k}\rangle|\mu_\sigma^k\rangle$  is recoverable and  $\hat{P}_{S+k} = \sum_\sigma |\nu_\sigma^k\rangle\langle\nu_\sigma^k|$ . To make  $\mathcal{R}^{(2)}$  a CPTP map, we add  $\hat{R}_{2S+1}^{(2)} = \hat{V}_{\text{res}}(\hat{I}_{\mathcal{H}} - \sum_{i=0}^{2S} \hat{P}_i)$  where  $\hat{I}_{\mathcal{H}}$  is the identity

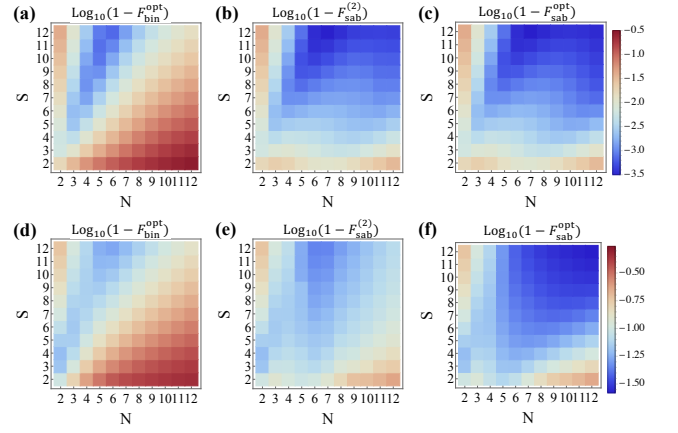


Figure 2. Channel infidelities (in logarithmic scale) for (a-c) **bin** code with optimal recovery, **sab** code with two-level recovery and **sab** code with optimal recovery, respectively, at  $\gamma = 0.1$ , and (d-f) same as (a-c) except for  $\gamma = 0.25$ . Each point represents a code with associated  $S$  and  $N$ .

operator on the entire Hilbert space and  $\hat{V}_{\text{res}}$  an arbitrary unitary acting on the complementary subspace of  $\{|\mu_\sigma\rangle\} \cup \{|\mu_\sigma^k\rangle\} \cup \{|\nu_\sigma^k\rangle\}$ .

To quantify the performance of  $\mathcal{E}$ , we use channel fidelity (aka. entanglement fidelity) defined as

$$F := \langle\Psi|\mathcal{I}_A \otimes \mathcal{E}_B(|\Psi\rangle\langle\Psi)|\Psi\rangle, \quad (10)$$

where  $\mathcal{I}_A$  is an identity channel on qubit A and  $|\Psi\rangle = \frac{1}{\sqrt{2}}(|0_A0_B\rangle + |1_A1_B\rangle)$  is a maximally entangled state of qubits A and B. In Fig. 2, we present the performance of  $\mathcal{R}^{(2)}$  and enhanced QEC capability of **sab**. At  $\gamma = 0.1$ , we compute the channel infidelities for **bin** codes undergoing  $\mathcal{N}_\gamma$  and optimal recovery  $\mathcal{R}^\circ$  (obtained from convex optimization [26, 35]) and, in comparison, those for **sab** codes undergoing  $\mathcal{R}^{(2)}$  and  $\mathcal{R}^\circ$ , respectively, after  $\mathcal{N}_\gamma$ . We note  $\mathcal{R}^\circ$  is considered here as it enables the best code performance, yet it is only restricted to be completely positive, trace preserving (CPTP) and can lack physics intuition and ease of implementation.

We see from Fig. 2(a) that, at  $\gamma = 0.1$ , desired **bin** codes are found along  $S \approx 2N$  while the entire  $N > S$  region features poor error protection. In comparison, as manifested in Fig. 2(b), **sab** codes with  $\mathcal{R}^{(2)}$  achieve much lower infidelities overall and open up the  $N > S$  region where destructive interference is pronounced. Fig. 2(c) shows the minimum channel infidelities for **sab** codes under  $\mathcal{R}^\circ$ . Comparing Fig. 2(b) and (c), we see that  $\mathcal{R}^{(2)}$  suffices to unleash the potential of **sab** at small  $\gamma$ , yielding infidelities close to optimal. The results also demystify  $\mathcal{R}^\circ$  for single-mode codes with parity – it is critical to capture the orthogonal component between partially overlapping error words. An alternative way to understand how SA helps suppress decoherence is to decompose effective QEC-protected qubit channel  $\mathcal{E}$  into Kraus operators [36]. As shown in Fig. 2(d-f), the advan-

tage of **sab** code becomes more significant at  $\gamma = 0.25$ , with the emergence of a new desired regime instead of  $S \approx 2N$ . Since  $\mathcal{R}^{(2)}$  only provides two layers of correction, it begins to perform sub-optimally in regions where  $\bar{n}\gamma \gtrsim S$  (or  $N\gamma \gtrsim 2$ ) at higher loss rate [Fig. 2(e)], indicating the need to resolve higher order error codewords or even consider the optimal recovery. Nonetheless, **sab** codes with  $\mathcal{R}^{(2)}$  still outperform **bin** codes with  $\mathcal{R}^o$ , offering a practically favorable and feasible QEC scheme.

**cat** code shares the parity structure with **bin** code and can be similarly enhanced (detailed in [36]). Specifically, two-component **cat** code [12], the simplest of the family which does not correct any excitation loss, will correct one loss approximately after SA is imposed. Same as **sab**, the SA can be implemented by  $\hat{U}_S$  while now  $2S$  is the number of coherent states in superposition – this explains why a small amount of cavity Kerr improves **cat**'s performance ([26], Fig. 9a).

*Optimality vs. complex noise* As it is not obvious that periodic SA is the *optimal* modification for **bin**, we relax the Kerr  $\hat{U}_K$  added to the encoding to be general (detailed in Sec. 3 of [36]). At large  $\gamma$  and  $N \gg S$  regimes, indeed we are able to find modified **bin** codes that further suppress the infidelities. These results point to the potential benefit of going beyond RCQC to consider generic phases in codeword designs [Fig. 1(c)].

To find the optimal encoding schemes given an error process, we deploy the technique energy-constrained [27] biconvex optimization of recovery and encoding for channel fidelity [28, 29]. Given the encoding and error channel  $\mathcal{N} \circ \mathcal{S}$ , computing optimal recovery  $\mathcal{S}^{-1} \circ \mathcal{R}$  to maximize channel fidelity is a convex problem, and vice versa. Using this technique, we can compute the optimal RCQCs and CCQCs given an error channel, respectively, to see if nontrivial phases are necessary in optimal code constructs [37].

For excitation loss, we find that optimal RCQCs and CCQCs are equivalent up to global rotations, indicating the redundancy of nontrivial phases [36]. The observation that neither channel imposes complex phases, reflected by their Kraus operators, confirms that the nature of error determines the role of phase in optimal code construction. To see where nontrivial phases play a role, we consider the joint channel of excitation loss and Kerr effect. The channel is relevant (e.g. in circuit QED systems) due to the concurrence of cavity Kerr and intrinsic loss. Kerr alone is reversible, but as it does not commute with  $\mathcal{N}_\gamma$ , randomness in the timing of excitation loss leads to uncertainty in phase  $\hat{U}_{K_r}$  imprints and thus decoherence [23]. The channel's superoperator [38] is

$$\mathcal{N}_{\gamma, Kt} = e^{-\frac{1}{2}iKt[\hat{n}^2, \cdot] - \ln(1-\gamma)(\hat{a} \cdot \hat{a}^\dagger - \frac{1}{2}\{\hat{n}, \cdot\})}. \quad (11)$$

In Table I we show the Wigner functions for the maximally mixed state  $\frac{1}{2}\hat{P}_{\text{code}}$ , which contains full information of a code, and the associated infidelities  $1 - F^o$  of the optimized RCQCs and CCQCs, respectively, at  $\gamma = 0.1$ ,

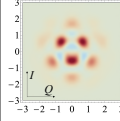
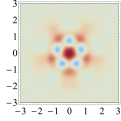
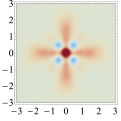
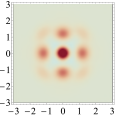
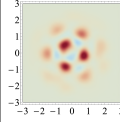
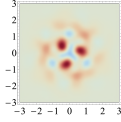
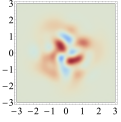
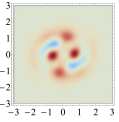
$Kt$	0	0.5	1	1.5
RCQCs	 6.1e-3	 1.4e-2	 2.5e-2	 3.6e-2
CCQCs	 6.1e-3	 1.2e-2	 2.3e-2	 3.2e-2
<b>bin</b> (2, 2)	1.8e-2	2.1e-2	3.0e-2	4.5e-2

Table I. Results from biconvex optimization under energy constraint  $\bar{n}_c = 2$  for single-mode RCQCs and CCQCs at  $\gamma = 0.1$  and different  $Kt$ . Wigner functions of maximally mixed state  $\frac{1}{2}\hat{P}_{\text{code}}$  are shown for the obtained optimal codes, respectively, with associated channel infidelities  $1 - F^o$  below them. The infidelities for **bin**(2, 2) are shown for comparison.

$\bar{n}_c = 2$  and various  $Kt$ . As a comparison we show the infidelities for **bin**(2, 2) with  $\bar{n} = 2$ , which protects against pure excitation loss [26]. For all  $Kt$ , both scenarios yield codes better than **bin**(2, 2), indicating the advantage of codes tailored to  $\mathcal{N}_{\gamma, Kt}$ . At  $Kt = 0$  (i.e. pure excitation loss) the optimized RCQC and CCQC are equivalent, as discussed earlier. For  $Kt \neq 0$ , nontrivial phases allow optimal CCQCs to offer better protection. The results exemplify the necessity of CCQCs for practical optimal QEC, as phase-imposing errors can often co-exist with other decoherence sources that they do not commute with.

*Sign-altered gkp and multi-qubit codes* So far, we have focused on codes defined in the Fock basis, while the same idea of phase engineering should apply to code constructs in other bases. For example, one can modify **gkp** code, defined in phase space for drift error [3], as follows

$$|\mu_\sigma\rangle = \sum_{s \in \mathbb{Z}} (-1)^\sigma |q = \alpha(\sigma + 2s)\rangle \quad (12)$$

where  $\sigma = 0, 1$  and  $2\alpha$  is the spacing between position eigenstates. Similar to **sab** and **sac**, the SA can be imposed by following the original **gkp** encoding procedure with  $e^{i\pi\hat{q}^2/4\alpha^2}$ , which transforms the **gkp** stabilizer  $\hat{S}_1 = e^{-ip\alpha}$  to  $\hat{S}'_1 = e^{-i(p-\pi q/2\alpha^2)\alpha}$  while leaving  $\hat{S}_2 = e^{2\pi iq/\alpha}$  unchanged. The new stabilizers define a nonrectangular **gkp** lattice, and for  $\alpha^2 = \sqrt{3}\pi/2$  it is hexagonal – the optimal packing in two dimensions with a larger-in-size smallest uncorrectable shift [3, 10].

The interference effects further extend into the multi-qubit regime. Consider Shor's [[9, 1, 3]] code that corrects arbitrary single-qubit Pauli errors with codewords  $|-\text{shor}\rangle \propto |\tilde{1}\tilde{0}\tilde{0}\rangle + |\tilde{0}\tilde{1}\tilde{0}\rangle + |\tilde{0}\tilde{0}\tilde{1}\rangle + |\tilde{1}\tilde{1}\tilde{1}\rangle$  and  $|+\text{shor}\rangle = \sigma_x^{\otimes 9}|-\text{shor}\rangle$ , where  $\tilde{i} = iii$  stands for blocks of three qubits. It detects weight-three  $\sigma_x$  errors, except for  $\sigma_x^{(i)}\sigma_x^{(i+1)}\sigma_x^{(i+2)}$  with  $i = 1, 4, 7$  as they are logical op-

erators. We now consider a sign-altered variant with  $|\text{-shor}'\rangle \propto |\tilde{1}00\rangle - |\tilde{0}10\rangle + |\tilde{0}01\rangle - |\tilde{1}11\rangle$  and  $|\text{+shor}'\rangle = |\text{+shor}\rangle$ . The new code detects  $\sigma_x^{(i)}\sigma_x^{(i+1)}\sigma_x^{(i+2)}$  and thus all weight-three  $\sigma_x$  errors. In addition, as detailed in [36], it detects more weight-three hybrid  $\sigma_x$  and  $\sigma_y$  errors while offers the same protection over  $\sigma_z$  as the original Shor code. A similar modification can improve Shor and Steane codes over qubit amplitude damping, which is a realistic concern for qubit systems [36, 39].

*Conclusion* In contrast to conventional designs of quantum codes whose error-correction capability comes from spanning codewords with distinct subsets of computational basis states, we explored the conjugate degree of freedom, the phases carried by basis states, to devise efficient quantum codes for various bosonic and qubit errors. The new codes can feature destructive interference and hence suppressed overlap between error codewords. To showcase the principle, we modify the codewords of bosonic binomial and cat codes that correct excitation loss errors by making certain probability amplitudes negative. With a quantum recovery that effectively captures the suppressed overlap, the modified codes demonstrate desired error-correction performance. For complex-valued noises, such as the joint channel of excitation loss and cavity Kerr, we show that considering complex-valued amplitudes in codewords is critical for optimal code constructs. The same principle also helps improve multi-qubit codes in overcoming noises such as Pauli errors and qubit amplitude damping. We expect the results developed here to deepen our understanding of quantum error correction and enable development of efficient quantum codes across a wide array of physical platforms for faithful quantum information processing.

*Acknowledgements* We thank Philippe Faist, Mengzhen Zhang, Sisi Zhou and Yuhui Ouyang for helpful discussions. We acknowledge supports from the ARL-CDQI (W911NF-15-2-0067, W911NF-18-2-0237), ARO (W911NF-18-1-0020, W911NF-18-1-0212), ARO MURI (W911NF-16-1-0349), AFOSR MURI (FA9550-14-1-0052, FA9550-15-1-0015), DOE (DE-SC0019406), NSF (EFMA-1640959), and the Packard Foundation (2013-39273).

- 
- [1] E. Knill, R. Laflamme, and G. J. Milburn, *Nature* **409**, 46 (2001).
- [2] S. L. Braunstein and P. van Loock, *Rev. Mod. Phys.* **77**, 513 (2005).
- [3] D. Gottesman, A. Kitaev, and J. Preskill, *Phys. Rev. A* **64**, 012310 (2001).
- [4] T. C. Ralph, A. Gilchrist, G. J. Milburn, W. J. Munro, and S. Glancy, *Phys. Rev. A* **68**, 042319 (2003).
- [5] I. L. Chuang, D. W. Leung, and Y. Yamamoto, *Phys. Rev. A* **56**, 1114 (1997).
- [6] D. W. Leung, M. A. Nielsen, I. L. Chuang, and Y. Yamamoto, *Phys. Rev. A* **56**, 2567 (1997).
- [7] Y. Ouyang, *Phys. Rev. A* **90**, 062317 (2014).
- [8] M. Bergmann and P. van Loock, *Phys. Rev. A* **94**, 012311 (2016).
- [9] M. Y. Niu, I. L. Chuang, and J. H. Shapiro, *Phys. Rev. A* **97**, 032323 (2018).
- [10] J. Harrington and J. Preskill, *Phys. Rev. A* **64**, 062301 (2001).
- [11] Z. Leghtas, G. Kirchmair, B. Vlastakis, R. J. Schoelkopf, M. H. Devoret, and M. Mirrahimi, *Phys. Rev. Lett.* **111**, 120501 (2013).
- [12] M. Mirrahimi, Z. Leghtas, V. V. Albert, S. Touzard, R. J. Schoelkopf, L. Jiang, and M. H. Devoret, *New J. Phys.* **16**, 045014 (2014).
- [13] N. Ofek, A. Petrenko, R. Heeres, P. Reinhold, Z. Leghtas, B. Vlastakis, Y. Liu, L. Frunzio, S. M. Girvin, L. Jiang, M. Mirrahimi, M. H. Devoret, and R. J. Schoelkopf, *Nature* **536**, 441 (2016).
- [14] M. Bergmann and P. van Loock, *Phys. Rev. A* **94**, 042332 (2016).
- [15] L. Li, C.-L. Zou, V. V. Albert, S. Muralidharan, S. M. Girvin, and L. Jiang, *Phys. Rev. Lett.* **119**, 030502 (2017).
- [16] M. H. Michael, M. Silveri, R. T. Brierley, V. V. Albert, J. Salmilehto, L. Jiang, and S. M. Girvin, *Phys. Rev. X* **6**, 031006 (2016).
- [17] L. Sun, A. Petrenko, Z. Leghtas, B. Vlastakis, G. Kirchmair, K. M. Sliwa, A. Narla, M. Hatridge, S. Shankar, J. Blumoff, L. Frunzio, M. Mirrahimi, M. H. Devoret, and R. J. Schoelkopf, *Nature* **511**, 444 (2014).
- [18] S. Krastanov, V. V. Albert, C. Shen, C.-L. Zou, R. W. Heeres, B. Vlastakis, R. J. Schoelkopf, and L. Jiang, *Phys. Rev. A* **92**, 040303 (2015).
- [19] R. W. Heeres, B. Vlastakis, E. Holland, S. Krastanov, V. V. Albert, L. Frunzio, L. Jiang, and R. J. Schoelkopf, *Phys. Rev. Lett.* **115**, 137002 (2015).
- [20] C. Shen, K. Noh, V. V. Albert, S. Krastanov, M. H. Devoret, R. J. Schoelkopf, S. M. Girvin, and L. Jiang, *Phys. Rev. B* **95**, 134501 (2017).
- [21] S. Lloyd and L. Viola, *Phys. Rev. A* **65**, 010101 (2001).
- [22] R. W. Heeres, P. Reinhold, N. Ofek, L. Frunzio, L. Jiang, M. H. Devoret, and R. J. Schoelkopf, *Nature Communications* **8**, 94 (2017).
- [23] L. Hu, Y. Ma, W. Cai, X. Mu, Y. Xu, W. Wang, Y. Wu, H. Wang, Y. Song, C. Zou, S. M. Girvin, L.-M. Duan, and L. Sun, [arXiv:1805.09072](https://arxiv.org/abs/1805.09072).
- [24] C. J. Axline, L. D. Burkhardt, W. Pfaff, M. Zhang, K. Chou, P. Campagne-Ibarcq, P. Reinhold, L. Frunzio, S. M. Girvin, L. Jiang, M. H. Devoret, and R. J. Schoelkopf, *Nature Physics* **14**, 705 (2018).
- [25] K. S. Chou, J. Z. Blumoff, C. S. Wang, P. C. Reinhold, C. J. Axline, Y. Y. Gao, L. Frunzio, M. H. Devoret, L. Jiang, and R. J. Schoelkopf, *Nature* **561**, 368 (2018).
- [26] V. V. Albert, K. Noh, K. Duivenvoorden, D. J. Young, R. T. Brierley, P. Reinhold, C. Vuillot, L. Li, C. Shen, S. M. Girvin, B. M. Terhal, and L. Jiang, *Phys. Rev. A* **97**, 032346 (2018).
- [27] K. Noh, V. V. Albert, and L. Jiang, *IEEE Transactions on Information Theory*, 1 (2018).
- [28] M. Reimpell and R. F. Werner, *Phys. Rev. Lett.* **94**, 080501 (2005).
- [29] R. L. Kosut and D. A. Lidar, *Quantum Information Processing* **8**, 443 (2009).

- [30] P. W. Shor, *Phys. Rev. A* **52**, R2493 (1995).
- [31] A. Steane, *Proceedings of the Royal Society of London. Series A: Mathematical, Physical and Engineering Sciences*, 452 (1996).
- [32] A. Kitaev, *Annals of Physics* **303**, 2 (2003).
- [33] C. H. Bennett, D. P. DiVincenzo, J. A. Smolin, and W. K. Wootters, *Phys. Rev. A* **54**, 3824 (1996).
- [34] E. Knill and R. Laflamme, *Phys. Rev. A* **55**, 900 (1997).
- [35] A. S. Fletcher, (2007), [arXiv:0706.3400](https://arxiv.org/abs/0706.3400) [quant-ph].
- [36] See Supplemental Material for more details.
- [37] We note that biconvex optimization does not guarantee globally optimality. The optimal codes are found via sampling across initial conditions.
- [38] Another format of Kerr contains a part linear in number operator. As phase rotation commutes with excitation loss (see Supplementary for details), the choice of format will not affect optimal code constructs.
- [39] A. S. Darmawan and D. Poulin, *Phys. Rev. Lett.* **119**, 040502 (2017).

# Designing good bosonic quantum codes via creating destructive interference – supplementary material

## I. EFFECTIVE QUBIT CHANNEL DECOMPOSITION

In this section, we examine the four Kraus operators of optimal effective qubit channels  $\mathcal{E}_{\text{bin}}^{\circ} = \mathcal{S}_{\text{bin}}^{-1} \circ \mathcal{R}_{\text{bin}}^{\circ} \circ \mathcal{N}_{\gamma} \circ \mathcal{S}_{\text{bin}}$  and  $\mathcal{E}_{\text{sab}}^{\circ} = \mathcal{S}_{\text{sab}}^{-1} \circ \mathcal{R}_{\text{sab}}^{\circ} \circ \mathcal{N}_{\gamma} \circ \mathcal{S}_{\text{sab}}$ , to visualize how SA leads to change in the leading error.

In Table I, we compare **bin** and **sab** with  $N = 4$ ,  $S = 3$  at  $\gamma = 0.1$ . We can see that the leading error for **bin** code with  $\mathcal{R}^{\circ}$  is a bit-flip error, resulted from events with more than  $S - 1$  losses. On the other side, **sab** code with  $\mathcal{R}^{\circ}$  reduces that bit-flip error by more than half – The remainder is turned into a  $\sigma_{+}$ -type error, as  $|\langle 1_{\text{sab}} | \hat{E}_k^{\dagger} \hat{E}_{S+k} | 0_{\text{sab}} \rangle|$  and  $|\langle 0_{\text{sab}} | \hat{E}_k^{\dagger} \hat{E}_{S+k} | 1_{\text{sab}} \rangle|$  in general differ due to the difference in basis state occupation profiles between  $|0_{\text{sab}}\rangle$  and  $|1_{\text{sab}}\rangle$ .

$\mathcal{E}_{\text{bin}}^{\circ}$		$\mathcal{E}_{\text{sab}}^{\circ}$	
Kraus operator	Prob.	Kraus operator	Prob.
$\begin{pmatrix} 0.99 & 0 \\ 0 & 0.99 \end{pmatrix}$	9.8e-1	$\begin{pmatrix} 1.0 & 0 \\ 0 & 0.99 \end{pmatrix}$	9.9e-1
$\begin{pmatrix} \mathbf{0} & \mathbf{-0.15} \\ \mathbf{-0.16} & \mathbf{0} \end{pmatrix}$	<b>2.4e-2</b>	$\begin{pmatrix} \mathbf{0} & \mathbf{-0.13} \\ \mathbf{-0.0098} & \mathbf{0} \end{pmatrix}$	<b>8.2e-3</b>
$\begin{pmatrix} -0.023 & 0 \\ 0 & 0.023 \end{pmatrix}$	5.3e-4	$\begin{pmatrix} 0 & -0.0031 \\ 0.040 & 0 \end{pmatrix}$	8.0e-4
$\begin{pmatrix} 0 & -0.0043 \\ 0.0040 & 0 \end{pmatrix}$	1.7e-5	$\begin{pmatrix} -0.028 & 0 \\ 0 & 0.028 \end{pmatrix}$	7.9e-4

Table I. Kraus operators (arranged in the descending order of probabilities) of the optimal effective qubit channel for **bin**(4, 3) and **sab**(4, 3) at  $\gamma = 0.1$ . The key difference between the two qubit channels, i.e. the suppression of bit-flip error, is highlighted in bold.

## II. FURTHER EXAMPLES OF SIGN ALTERATION

### A. Modified cat code for excitation loss

Consider the simplest **cat** code  $|\sigma_{\text{cat}}\rangle \propto \sum_{n=0}^{\infty} \frac{\alpha^{2n+\sigma}}{\sqrt{(2n+\sigma)!}} |2n+\sigma\rangle$  for  $\sigma \in \{0, 1\}$ . This PCQC cannot detect even a single loss event  $\hat{a}$ , as  $\hat{a}|1_{\text{cat}}\rangle \propto |0_{\text{cat}}\rangle$  and visa versa. However, a simple modification produces the sign-altered **cat** (**sac**) codewords  $|\sigma_{\text{sac}}\rangle \propto \sum_{n=0}^{\infty} \frac{\alpha^{2n+\sigma}}{\sqrt{(2n+\sigma)!}} (-1)^{\sigma+1} |2n+\sigma\rangle$  that do not significantly overlap upon a loss event. While  $\hat{a}|1_{\text{sac}}\rangle$  is still in the support of  $|0_{\text{sac}}\rangle$  (i.e., in the even Fock state subspace), the overlap between  $\hat{a}|1_{\text{sac}}\rangle$  and  $|0_{\text{sac}}\rangle$  is exponentially suppressed with  $\alpha$  due to *destructive interference*. Thus, SA can extend a **cat** code that does not correct a loss error to one that approximately does. This behavior can also be understood in terms of bosonic coherent states  $|\alpha\rangle$  (with  $\hat{a}|\alpha\rangle = \alpha|\alpha\rangle$ ). In this basis,  $|0_{\text{sac}}\rangle \propto |i\alpha\rangle + |-i\alpha\rangle$ ,  $|1_{\text{sac}}\rangle \propto |\alpha\rangle - |-\alpha\rangle$ , and  $\langle 0_{\text{sac}} | \hat{a} | 1_{\text{sac}} \rangle \rightarrow 0$  since the coherent states of  $|0_{\text{sac}}\rangle$  are well separated from those of  $\hat{a}|1_{\text{sac}}\rangle$ .

Generically, the codewords of **cat** codes are cat states, superpositions of  $2S$  coherent states lying equidistantly on a circle in the phase space Li *et al.* [1]. In Fock basis, they can be expressed as

$$|C_{\alpha}^n\rangle = \sqrt{\frac{2S}{\mathcal{N}_{\alpha}^n}} \sum_{m=0}^{\infty} \frac{e^{-\frac{\alpha^2}{2}} \alpha^{n+2mS}}{\sqrt{(n+2mS)!}} |n+2mS\rangle \quad (1)$$

where  $n = 0, 1, \dots, 2S - 1$ ,  $\mathcal{N}_{\alpha}^n = 2S \langle \alpha | \hat{\Pi}_{n \bmod S} | \alpha \rangle$  is the normalization factor, and  $\lim_{\alpha \rightarrow \infty} \mathcal{N}_{\alpha}^n = 1$ . Without losing generality,  $\alpha$  is assumed to be real here and we choose the  $\text{Span}\{|C_{\alpha}^0\rangle, |C_{\alpha}^S\rangle\}$  to be the logical subspace – for **cat** codes there is freedom on the choice of “ $d$ -subspace”,  $\text{Span}\{|C_{\alpha}^d\rangle, |C_{\alpha}^{d+S}\rangle\}$  as the logical subspace (Li *et al.* [1]).

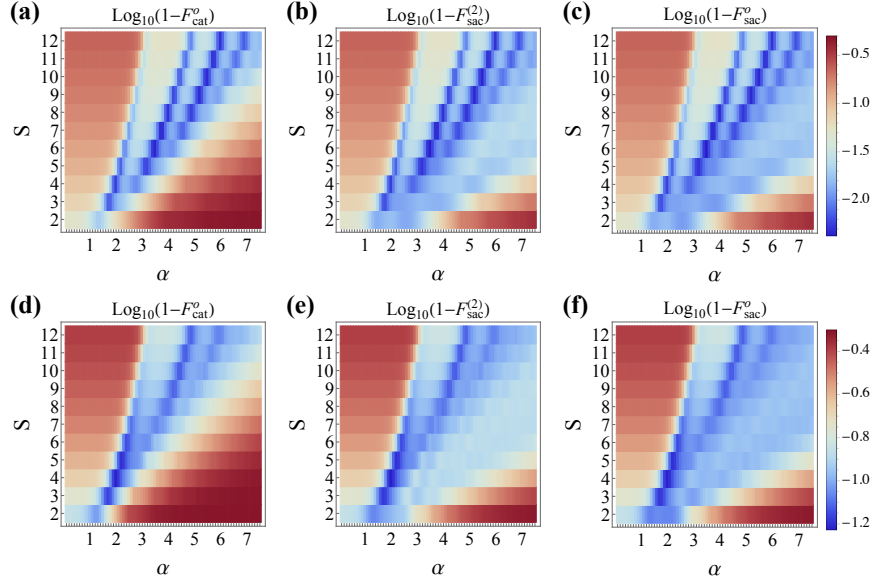


Figure 1. Channel infidelities (in logarithmic scale) for (a-c) **cat** code with optimal recovery (as indicated by the superscript), **sac** code with two-level recovery and **sac** code with optimal recovery, respectively, at  $\gamma = 0.1$ , and (d-f) same as (a-c) except for  $\gamma = 0.25$ . Each point represents a code with associated  $S$  and  $\alpha$ .

Generic **sac** code is defined as follows

$$|0_{\text{sac}}\rangle = \sqrt{\frac{2S}{\mathcal{N}_\alpha^0}} \sum_{m=0}^{\infty} (-1)^m \frac{e^{-\frac{\alpha^2}{2}} \alpha^{2mS}}{\sqrt{2mS!}} |2mS\rangle, \quad (2)$$

$$|1_{\text{sac}}\rangle = \sqrt{\frac{2S}{\mathcal{N}_\alpha^S}} \sum_{m=0}^{\infty} \frac{e^{-\frac{\alpha^2}{2}} \alpha^{(2m+1)S}}{\sqrt{(2m+1)S!}} |(2m+1)S\rangle. \quad (3)$$

The above codewords can be generated in the same way as **sab** code, i.e.  $\mathcal{S}_{\text{sac}}(\cdot) = \hat{U}_S \mathcal{S}_{\text{cat}}(\cdot) \hat{U}_S^\dagger$ . We can see from Fig. 1 that for **sac** the  $\alpha^2 \gamma \approx S$  region is opened up due to the additional suppression of errors induced by  $S$  to  $2S-1$  losses. For small loss,  $\mathcal{R}^{(2)}$  yields QEC performance close to optimal. Unlike **bin** codes, at finite  $\alpha$ , the performance of **cat** codes is also constrained by dephasing caused by  $\langle 0_{\text{sac}} | \hat{n}^m | 0_{\text{sac}} \rangle \neq \langle 1_{\text{sac}} | \hat{n}^m | 1_{\text{sac}} \rangle$  for  $m \in \mathbb{Z}^+$ . This is why at low loss rates the optimal codes are found around “sweet spots” that are specific choices of  $\alpha$  minimizing the dephasing (Li *et al.* [1]). As a result, SA that suppresses bit-flip type of decoherence cannot bring improvement in QEC performance as significant as it does for **bin** codes.

## B. Modified Shor’s $[[9, 1, 3]]$ code for Pauli errors

Given a code with projection  $P$  and error  $E$ , the error is said to be *detectable* if  $PEP \propto P$ . A set of errors  $\mathbb{E} = \{E\}$  is said to be *correctable* if  $PE^\dagger FP \propto P$  for all  $E, F \in \mathbb{E}$ . Here we showcase a sign-altered variant of Shor code that better protects against Pauli errors.

With stabilizers  $\sigma_z^{(1)} \sigma_z^{(2)}, \sigma_z^{(2)} \sigma_z^{(3)}, \sigma_z^{(4)} \sigma_z^{(5)}, \sigma_z^{(5)} \sigma_z^{(6)}, \sigma_z^{(7)} \sigma_z^{(8)}, \sigma_z^{(8)} \sigma_z^{(9)}, \sigma_x^{(1)} \sigma_x^{(2)} \sigma_x^{(3)} \sigma_x^{(4)} \sigma_x^{(5)} \sigma_x^{(6)}$  and  $\sigma_x^{(4)} \sigma_x^{(5)} \sigma_x^{(6)} \sigma_x^{(7)} \sigma_x^{(8)} \sigma_x^{(9)}$ , Shor code

$$\begin{cases} |+\text{shor}\rangle &= \frac{1}{2}(|000\ 000\ 000\rangle + |000\ 111\ 111\rangle + |111\ 000\ 111\rangle + |111\ 111\ 000\rangle) \\ |-\text{shor}\rangle &= \frac{1}{2}(|111\ 000\ 000\rangle + |000\ 111\ 000\rangle + |000\ 000\ 111\rangle + |111\ 111\ 111\rangle) \end{cases} \quad (4)$$

corrects arbitrary single-qubit errors. For two-qubit errors, the code only offers partial correction as  $\sigma_x^{(i)} \sigma_x^{(i+1)} \sigma_x^{(i+2)}$  with  $i = 1, 4, 7$  are logical  $\sigma_x$  operators. We then consider the following modified Shor code

$$\begin{cases} |+\text{shor}'\rangle &= \frac{1}{2}(|000\ 000\ 000\rangle - |000\ 111\ 111\rangle + |111\ 000\ 111\rangle - |111\ 111\ 000\rangle) \\ |-\text{shor}'\rangle &= \frac{1}{2}(|111\ 000\ 000\rangle + |000\ 111\ 000\rangle + |000\ 000\ 111\rangle + |111\ 111\ 111\rangle) \end{cases}. \quad (5)$$



The stabilizer set of this code consists of the same six  $\sigma_z$  stabilizers as Shor code,  $\sigma_x^{(1)}\sigma_x^{(2)}\sigma_x^{(3)}\sigma_x^{(7)}\sigma_x^{(8)}\sigma_x^{(9)}$  and  $\sigma_y^{(1)}\sigma_x^{(2)}\sigma_x^{(3)}\sigma_y^{(4)}\sigma_x^{(5)}\sigma_x^{(6)}\sigma_z^{(7)}$ . Its logical operators are  $\bar{\sigma}_x = \sigma_z^{\otimes 9}$  and  $\bar{\sigma}_z = \sigma_x^{(1)}\sigma_x^{(2)}\sigma_x^{(3)}\sigma_z^{(4)}$ , which is now weight-four. Same as Shor code, the modified code corrects arbitrary single-qubit and detects arbitrary two-qubit Pauli errors. In addition, one can see that

$$\begin{cases} \sigma_x^{(1)}\sigma_x^{(2)}\sigma_x^{(3)}|+\text{shor}'\rangle &= \frac{1}{2}(|111\ 000\ 000\rangle - |000\ 111\ 000\rangle + |000\ 000\ 111\rangle - |111\ 111\ 111\rangle) \\ \sigma_x^{(1)}\sigma_x^{(2)}\sigma_x^{(3)}|-\text{shor}'\rangle &= \frac{1}{2}(|000\ 000\ 000\rangle + |000\ 111\ 111\rangle + |111\ 000\ 111\rangle + |111\ 111\ 000\rangle) \end{cases}, \quad (6)$$

which leads to  $P\sigma_x^{(1)}\sigma_x^{(2)}\sigma_x^{(3)}P = 0$ . In fact, the code now detects  $E = \sigma_x^{(i)}\sigma_x^{(i+1)}\sigma_x^{(i+2)}$  for  $i = 1, 4, 7$  and hence all weight-three  $\sigma_x$  errors. Similarly, one can check that fewer weight-three hybrid  $\sigma_x$  and  $\sigma_y$  errors are now undetectable. For error correction, one can also design recoveries capture the additional QEC matrix elements that are now zero. The trade-off for the improved error detection/correction is that the new code is no longer a CSS code.

### C. Modified Shor's $[[9, 1, 3]]$ code and Steane's $[[7, 1, 3]]$ code for qubit amplitude damping

For single-qubit amplitude damping channel with rate  $\gamma$ , the Kraus operators are

$$A_0 = I + \left(\sqrt{1-\gamma} - 1\right)\sigma_+\sigma_- \quad \text{and} \quad A_1 = \sqrt{\gamma}\sigma_- \quad (7)$$

where  $\sigma_- = |0\rangle\langle 1| = \sigma_+^\dagger$ .

Consider correction of qubit amplitude damping errors with Shor code in Eq. 4. The logical codewords can be conveniently expressed as  $|-\rangle \propto |\tilde{1}\tilde{0}\tilde{0}\rangle + |\tilde{0}\tilde{1}\tilde{0}\rangle + |\tilde{0}\tilde{0}\tilde{1}\rangle + |\tilde{1}\tilde{1}\tilde{1}\rangle$  and  $|+\text{shor}\rangle = \sigma_x^{\otimes 9}|-\text{shor}\rangle$  where  $\tilde{iii}$  stands for blocks of three qubits. The code detects arbitrary two-qubit damping errors and ceases to protect some of the three-qubit errors, such as  $\tilde{\sigma}_-^{(i)} = \sigma_-^{(i)}\sigma_-^{(i+1)}\sigma_-^{(i+2)}$  for  $i \in \{1, 4, 7\}$  and  $\sigma_-^{(i)} = |0\rangle_i\langle 1|_i$ . Now consider the modified codeword  $|-\text{shor}''\rangle \propto |\tilde{1}\tilde{0}\tilde{0}\rangle + |\tilde{0}\tilde{1}\tilde{0}\rangle + |\tilde{0}\tilde{0}\tilde{1}\rangle - |\tilde{1}\tilde{1}\tilde{1}\rangle$ . Taking  $i = 1$  as an example,  $\tilde{\sigma}_-^{(1)}|-\text{shor}''\rangle \propto |\tilde{0}\tilde{0}\tilde{1}\rangle - |\tilde{0}\tilde{1}\tilde{1}\rangle$  then does not overlap with  $|+\text{shor}''\rangle = |+\text{shor}\rangle$ . While such errors cannot be fully detected as  $\langle -_{\text{code}}|\tilde{\sigma}_-^{(i)}|+_{\text{code}}\rangle \neq 0$  for both versions of the code, it is possible to capture the enhancement with an analogous ‘‘two-level’’ quantum recovery developed for those single-mode codes.

Similarly, we can modify the logical codewords of Steane code by altering the coefficient of the  $|111111\rangle$  computational basis state from  $+1$  to  $-1$ :

$$\begin{cases} |0_{\text{stn}'}\rangle &= \frac{1}{\sqrt{8}}(|0000000\rangle + |1010101\rangle + |0110011\rangle + |1100110\rangle + |0001111\rangle + |1011010\rangle + |0111100\rangle + |1101001\rangle) \\ |1_{\text{stn}'}\rangle &= \frac{1}{\sqrt{8}}(-|1111111\rangle + |0101010\rangle + |1001100\rangle + |0011001\rangle + |1110000\rangle + |0100101\rangle + |1000011\rangle + |0010110\rangle) \end{cases}. \quad (8)$$

Just like the original Steane code,  $\text{stn}'$  can provably correct arbitrary single-qubit Pauli errors. Since a larger set of weight-three errors is now not completely detectable,  $\text{stn}'$  is a worse-performing code against local Pauli noise. However, it is slightly better-performing when it comes to qubit amplitude damping.

Both the Steane code and  $\text{stn}'$  correct one amplitude damping error and fail to correct two losses in the same way. A difference occurs when it comes to three-loss errors  $\sigma_-^{(i)}\sigma_-^{(j)}\sigma_-^{(k)}$ : Such errors become detectable for  $\text{stn}'$  as, for example,  $\sigma_-^{(2)}\sigma_-^{(4)}\sigma_-^{(6)}|1_{\text{stn}'}\rangle \propto -|1010101\rangle + |0000000\rangle$ , which is orthogonal to  $|0_{\text{stn}'}\rangle$ . The same occurs for  $\{i, j, k\} = \{1, 4, 5\}, \{3, 4, 7\}$ , and five other combinations corresponding to the five remaining basis elements of  $|1_{\text{stn}'}\rangle$ . The remaining possible loss triples annihilate both  $|0_{\text{stn}'}\rangle$  and  $|1_{\text{stn}'}\rangle$ . Therefore, all loss triples are detectable. However, the modification does not improve the code against two-loss errors, and we observe that the channel fidelity (calculated using a numerical optimal recovery) improves at most in the third decimal place.

## III. GENERIC KERR HAMILTONIAN FOR ENCODING

Given  $N$ ,  $S$  and  $K$ , the encoding isometry  $\hat{U}_K\mathcal{S}_{\text{bin}}(\cdot)\hat{U}_K^\dagger$  defines a new variant of  $\text{bin}$  under Kerr. Dependent on  $\gamma$ , one can scan over  $K$  to numerically maximize  $F^\circ$  of the new code. We denote the variant that generates the highest channel fidelity as optimal-Kerr binomial ( $\text{okb}$ ) code. In Fig. 2, we compare  $\log_{10}(1 - F_{\text{sab}}^\circ)$  and  $\log_{10}(1 - F_{\text{okb}}^\circ)$  at  $\gamma = 0.1$  and  $\gamma = 0.25$ , respectively. We can see that the difference emerges in the  $N \gg S$  region as  $\gamma$  gets larger. In that region, each code word is spanned by a large number of Fock states (proportional to  $N$ ), and a simple SA becomes suboptimal for creating destructive interference between error words. We note that a similar preprocessing – Gaussian presqueezing – has been found to improve the fidelity of pure non-Gaussian states after lossy transmission (Filip [2], Le Jeannic *et al.* [3]).

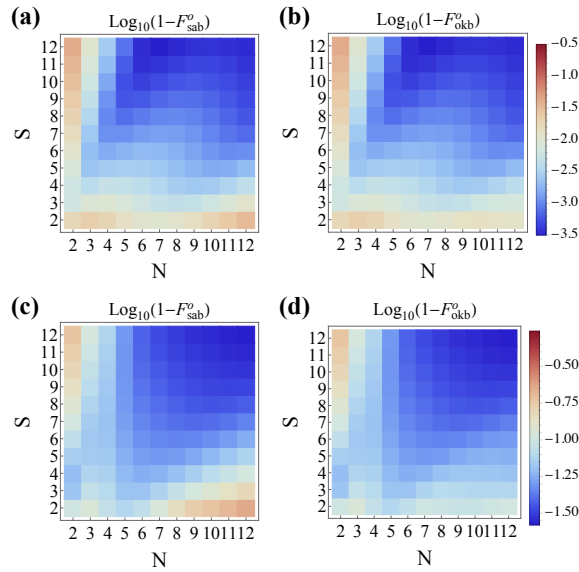


Figure 2. Channel infidelities (in logarithmic scale) from optimal recovery for **sab** and **okb** codes, respectively, at (a-b)  $\gamma = 0.1$  and (c-d)  $\gamma = 0.25$ . Each point represents a code with associated  $S$  and  $N$ . Please note the color scale is changed.

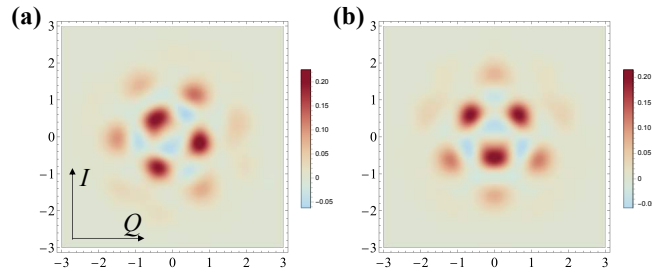


Figure 3. Optimal codes from biconvex optimization under energy constraint  $\bar{n}_c = 2$  for excitation loss channel. (a) Optimal CCQC for excitation loss channel with  $\gamma = 0.1$ . (b) The CCQC in (a) after a phase rotation that reduces it to a RCQC.

#### IV. OPTIMAL BOSONIC CODES FOR EXCITATION LOSS AND DEPHASING CHANNEL

We consider the optimal bosonic codes for excitation loss channel. Since the excitation loss channel  $\mathcal{N}_\gamma$ , with Kraus operator  $\hat{E}_k = \sqrt{\frac{\gamma^k}{k!}}(1-\gamma)^{\frac{\hat{n}}{2}}\hat{a}^k$ , commutes with phase rotation  $V_\theta = e^{i\theta\hat{n}}$

$$\mathcal{N}_\gamma(V_\theta\rho V_\theta^\dagger) = V_\theta\mathcal{N}_\gamma(\rho)V_\theta^\dagger, \quad (9)$$

one can apply any phase rotation to  $\frac{1}{2}\hat{P}_{\text{code}}$ , which fully characterizes the encoding subspace, and obtain a new code with the same QEC performance as  $V_\theta$  can always be absorbed into recovery  $\mathcal{R}$ . In Fig. 3a, we plot the Wigner functions for the maximally mixed state  $\frac{1}{2}\hat{P}_{\text{code}}$  of the optimal CCQC for excitation loss with  $\gamma = 0.1$  and  $\bar{n}_c = 2$ . We find that, with a proper  $V_\theta$ , as shown in Fig. 3b, one can obtain a new code with Wigner function of  $\frac{1}{2}\hat{P}_{\text{code}}$  symmetric against Q-axis, i.e. all density matrix entries are real. The new code is an RCQC, indicating the redundancy of nontrivial phases in optimal code constructs for excitation loss. We note that this redundancy of phase does not seem to be lifted as we consider qudit ( $d \geq 3$ ) codes. In Fig. 5a in Noh *et al.* [4], Wigner functions of  $\frac{1}{d}\hat{P}_{\text{code}}$  of optimized qudit codes ( $2 \leq d \leq 5$ ) for the excitation loss channel with  $\gamma = 0.1$  are computed. For all  $d$ 's considered, the Wigner functions are in hexagonal lattice which, upon proper phase rotations, will become symmetric against Q-axis and hence represent a RCQC. These findings indicate that the necessity of phase in optimal code constructs

solely depends on the nature of channel, not the dimension of encoding.

---

- [1] L. Li, C.-L. Zou, V. V. Albert, S. Muralidharan, S. M. Girvin, and L. Jiang, *Phys. Rev. Lett.* **119**, 030502 (2017).
- [2] R. Filip, *Phys. Rev. A* **87**, 042308 (2013).
- [3] H. Le Jeannic, A. Cavailles, K. Huang, R. Filip, and J. Laurat, *Phys. Rev. Lett.* **120**, 073603 (2018).
- [4] K. Noh, V. V. Albert, and L. Jiang, *IEEE Transactions on Information Theory* , 1 (2018).